J. Austral. Math. Soc. Ser. B 30(1988), 127–146

THE KELVIN IMPULSE: APPLICATION TO CAVITATION BUBBLE DYNAMICS

J. R. BLAKE[1]

(Received 11 September 1987; revised 2 February 1988)

Abstract

The Kelvin impulse is a particularly valuable dynamical concept in unsteady fluid mechanics, with Benjamin and Ellis [2] appearing to be the first to have realised its value in cavitation bubble dynamics. The Kelvin impulse corresponds to the apparent inertia of the cavitation bubble and, like the linear momentum of a projectile, may be used to determine aspects of the gross bubble motion, such as the direction of movement of the bubble centroid.

It is defined as

$$\mathbf{I} = \rho \int_S \phi \mathbf{n}\, dS,$$

where ρ is the fluid density, ϕ is the velocity potential, S is the surface of the cavitation bubble and $\mathbf{n}$ is the outward normal to the fluid. Contributions to the Kelvin impulse may come from the presence of nearby boundaries and the ambient velocity and pressure field. With this number of mechanisms contributing to its development, the Kelvin impulse may change sign during the lifetime of the bubble. After collapse of the bubble, it needs to be conserved, usually in the form of a ring vortex. The Kelvin impulse is likely to provide valuable indicators as to the physical properties required of boundaries in order to reduce or eliminate cavitation damage. Comparisons are made against available experimental evidence.

1. Introduction

The Kelvin impulse, as one might anticipate, has the dimensions of momentum. It is related to the concept of impulse in particle mechanics, an analogy that is exploited later. However, care needs to be exercised in relating it to the change in momentum from one instant to the next, because of the possible unbounded

[1]Department of Mathematics, University of Wollongong, Wollongong, N.S.W. 2500 Australia.

nature of the fluid that may occur in theoretical fluid mechanics. Perhaps because of this indefinite nature of the impulse, it has not been exploited as fully as it should have been. Lamb [9] has a number of comments to make about the impulse, stating:

"*whatever the motion of the solid and fluid at any instant, it might be generated instantaneously from rest by a properly adjusted impulsive wrench*".

Later on he says:

"*the wrench is in fact that which would be required to counteract the impulsive pressure on the surface*", and later again: "*Kelvin called this the 'impulse' of the system under consideration*"

Many years later Benjamin and Ellis [2] stated:

"*... again if the liquid remained simply connected as the cavity closed up, the Kelvin impulse would have to vanish, which we cannot allow in the absence of an external retarding force. Thus the cavity must deform in such a way as to make the liquid multiply connected—circulation can then appear in the liquid and we are left in the limit with a vortex system possessing the original Kelvin impulse*"

And from the same paper, another quote:

"*One should always reason in terms of the Kelvin impluse, not in terms of the fluid momentum...*"

The Kelvin impulse corresponds to the apparent inertia of a cavitation bubble and, like the linear momentum of a particle, may be used to determine aspects of the gross bubble motion such as the movement of the bubble centroid. Thus, from this perspective, the study of a cavitating liquid can be reduced to modelling collectively the behaviour of the individual bubbles, a very great simplification.

The concept of the Kelvin impulse is introduced by considering an impulse from particle mechanics in the next section, followed by a section which develops the ideas of the Kelvin impulse in a semi-infinite fluid. A relation is obtained between the Kelvin impulse and a momentum flux-like term on the half-space boundary. These ideas may be extended to a finite number of bubbles next to the boundary. It is also possible to relate the motion of the centroid of the bubble to the Kelvin impulse in several selected examples. In the far-field we can approximate the fluid motion due to a cavitation bubble by a source or a source and a dipole combination. This representation may be exploited to yield the Kelvin impulse, by an analytic integration on the half-space boundary. This yields further information and valuable insight into the interaction mechanics of cavitation bubbles near boundaries. Some of these predictions will be related to examples of experimental observation.

2. Impulse in particle mechanics

If a force F of variable magnitude acts on a particle of constant mass m we have, from Newton's second law of motion, that

$$F = m\frac{dv}{dt}, \tag{2.1}$$

where v is the velocity and t is time, and when integrated from $(0, t)$, this yields

$$I = \int_0^t F\,dt = mv(t) - mv(0). \tag{2.2}$$

The quantity $\int_0^t F\,dt$ is known as the impulse I and represents the change in momentum of the particle along the line of action of the force. If the particle starts from rest, the impulse is the actual momentum of the particle at time t, i.e.

$$I = \int_0^t F\,dt = mv(t). \tag{2.3}$$

This result may be generalised further still by allowing the mass to also be a function of time $m(t)$, a factor of some relevance later when we consider the added mass of a cavitation bubble, which will clearly be a function of time because of the changing volume of the bubble. It should also be noted at this stage that the sign of I in (2.3) determines the direction of translation of the particle, a factor that is exploited in later sections.

We now develop similar ideas for a liquid.

3. The Kelvin impulse

The Kelvin impulse for a cavitation bubble in a liquid is defined as, [3],

$$\mathbf{I} = \rho \int_s \phi \mathbf{n}\,dS, \tag{3.1}$$

where ρ is the fluid density, ϕ is the velocity potential, S the surface of the cavitation bubble and $\mathbf{n}$ is the outward normal to the fluid (i.e. into the bubble - see Figure 1). This expression arises naturally from consideration of the conservation of momentum in an inviscid incompressible fluid moving irrotationally.

Because the liquid is incompressible, conservation of mass requires that the velocity field $\mathbf{u}$ be solenoidal, i.e.

$$\nabla \cdot \mathbf{u} = 0, \tag{3.2}$$

while the motion being irrotational yields

$$\nabla \times \mathbf{u} = 0, \tag{3.3}$$

https://doi.org/10.1017/S0334270000006111 Published online by Cambridge University Press

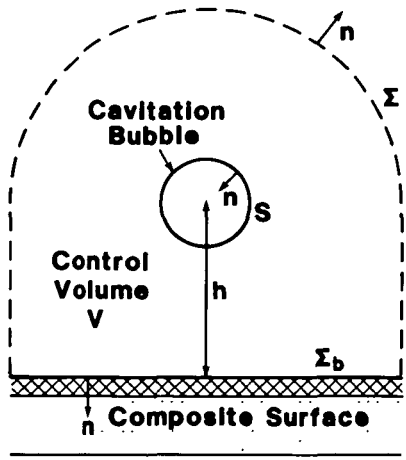

FIGURE 1. Illustrates the half space control volume near a 'composite' boundary that is used in determining relations for the Kelvin impulse.

such that the velocity may be represented by the gradient of a potential ϕ as

$$\mathbf{u} = \nabla\phi. \tag{3.4}$$

Combining (3.4) and (3.2) yields the field equation as Laplace's equation:

$$\nabla^2\phi = 0. \tag{3.5}$$

Purely inviscid flow leads to the pressure being expressed by the Bernoulli expression,

$$p = p_0 - \rho\frac{\partial\phi}{\partial t} - \frac{1}{2}\rho|\mathbf{u}|^2. \tag{3.6}$$

Equation (3.6) could be generalised by the inclusion of the hydrostatic pressure term, but at this stage we wish to restrict our analysis to the inertial aspects of the fluid motion. The above equations are what may be called "point-wise" equations, i.e. are valid at every point in the fluid. However, much valuable information may be obtained from global balances as against local balances above. This naturally leads us to the next section on the global conservation of linear momentum.

4. Global conservation of linear momentum

Let us consider a finite control volume V of fluid bounded by a bubble, the half-space boundary Σ_b and the material control surface Σ within the liquid (see Figure 1). The linear momentum of the volume of liquid in this fixed frame of reference is represented by

$$\mathbf{P} = \rho\int_V \mathbf{u}\,dV, \tag{4.1}$$

https://doi.org/10.1017/S0334270000006111 Published online by Cambridge University Press

which, on the use of the Gauss divergence theorem, may be equated to

$$\begin{aligned}\mathbf{P} &= \rho \int_{S\cup\Sigma\cup\Sigma_b} \phi \mathbf{n}\, dS \\ &= \rho \left\{ \int_S \phi \mathbf{n}\, dS + \int_{\Sigma\cup\Sigma_b} \phi \mathbf{n}\, dS \right\}.\end{aligned} \tag{4.2}$$

It can now be seen how the Kelvin impulse arises naturally in this study, for it is the first term on the right of equation (4.2). It is also clear that the second integral is not well specified for an infinite or semi-infinite fluid, since $\phi = O(1/R)$ and $dS = O(R^2)$.

The apparent problems may be circumvented if we consider the rate of change of momentum in the finite material control volume by equating this to the pressure forces acting at the boundaries, i.e.

$$\frac{d\mathbf{P}}{dt} = -\int_{S\cup\Sigma\cup\Sigma_b} p\mathbf{n}\, dS. \tag{4.3}$$

Since all the integrals are finite, it is expeditious to break the momentum up into the Kelvin impulse and the remaining integral over the control surface and boundary. Thus we have

$$\frac{d\mathbf{I}}{dt} = -\int_{S\cup\Sigma\cup\Sigma_b} p\mathbf{n}\, dS - \frac{d}{dt}\int_{\Sigma\cup\Sigma_b} \phi \mathbf{n}\, dS. \tag{4.4}$$

Now for a cavitation bubble the saturated vapour pressure inside the bubble is constant which leads to a null contribution to the right hand side of (4.4) from the surface integral over S. On exploiting the Bernoulli pressure condition and the Reynolds transport theorem, we may write (4.4) as

$$\frac{d\mathbf{I}}{dt} = \rho \int_{\Sigma\cup\Sigma_b} \left(\frac{1}{2}(\nabla\phi)^2 \mathbf{n} - \frac{\partial\phi}{\partial n}\nabla\phi \right) dS. \tag{4.5}$$

Equation (4.5) is now in a suitable form to allow the control surface Σ to extend out to infinity because the integral is $O(R^{-4})$ leading to zero contribution in the limit.

Thus on integration we have a very similar expression to the elementary particle mechanics expression in (2.3) of

$$\mathbf{I} = \int_S \phi \mathbf{n}\, dS = \mathbf{I}_0 + \int_0^t \mathbf{F}(t)\, dt, \tag{4.6}$$

where $\mathbf{I}_0$ is the initial Kelvin impulse and

$$\mathbf{F}(t) = \rho \int_{\Sigma_b} \left\{ \frac{1}{2}(\nabla\phi)^2 \mathbf{n} - \frac{\partial\phi}{\partial n}\nabla\phi \right\} dS. \tag{4.7}$$

If we were to include buoyancy forces, (4.7) would be modified by the addition of $\rho g V(t) \cos\theta$ to the RHS, where g is the gravitational acceleration, $V(t)$, the

https://doi.org/10.1017/S0334270000006111 Published online by Cambridge University Press

bubble volume and θ is the angle between the gravity vector and the outward normal to the half-space boundary.

The theory may also be extended to N bubbles, yielding

$$\mathbf{I} = \sum_{n=1}^{N} \mathbf{I}_n = \rho \sum_{n=1}^{N} \int_{S_n} \phi \mathbf{n}\, dS. \tag{4.8}$$

The relations (4.6) and (4.7) will still hold provided the potential ϕ is now the sum of the contributions from all the bubbles, i.e.

$$\phi = \sum_{n=1}^{N} \phi_n. \tag{4.9}$$

5. Motion of the bubble centroid in an infinite fluid

If we represent the volume of the bubble, surface S, by D, then the position vector $\mathbf{x}_c$ for the centroid may be written as

$$\mathbf{x}_c = \frac{1}{V_b} \int_D \mathbf{x}\, dV, \tag{5.1}$$

where V_b is the volume of the bubble. If we consider the rate of change of $V_b \mathbf{x}_c$ with time, we arrive at the following:

$$\frac{d(V_b \mathbf{x}_c)}{dt} = \frac{d}{dt} \int_D \mathbf{x}\, dV, \tag{5.2}$$

which on applying the Reynolds transport theorem yields

$$\frac{d}{dt}(V_b \mathbf{x}_c) = -\int_S \mathbf{s} \frac{\partial \phi}{\partial n}\, dS, \tag{5.3}$$

where $\mathbf{s}$ is the position vector of a point on S (see also [10]).

Green's formula for the potential in an infinite fluid is

$$\phi = \frac{1}{4\pi} \int_s \left(\frac{\partial \phi}{\partial n} \frac{1}{r} - \phi \frac{\partial}{\partial n} \left(\frac{1}{r} \right) \right) dS, \tag{5.4}$$

where $r = |\mathbf{x} - \mathbf{s}|$, noting the definition of the normal $\mathbf{n}$. In the far-field where $|\mathbf{x}|$ is much greater than $|\mathbf{s}|$, we may approximate the following expressions in the integral, as in [10]:

$$\frac{1}{|\mathbf{x} - \mathbf{s}|} = \frac{1}{|\mathbf{x}|} + \frac{\mathbf{s} \cdot \mathbf{x}}{|\mathbf{x}|^3} + O\left(\frac{1}{|\mathbf{x}|^3} \right), \tag{5.5}$$

and

$$\begin{aligned} \frac{\partial}{\partial n} \left(\frac{1}{|\mathbf{x} - \mathbf{s}|} \right) &= \mathbf{n} \cdot \nabla_s \frac{1}{|\mathbf{x} - \mathbf{s}|} \\ &= \frac{\mathbf{n} \cdot \mathbf{x}}{|\mathbf{x}|^3} + O\left(\frac{1}{|\mathbf{x}|^3} \right). \end{aligned} \tag{5.6}$$

https://doi.org/10.1017/S0334270000006111 Published online by Cambridge University Press

Thus in the far-field the potential behaves like

$$\phi \sim \frac{1}{4\pi|\mathbf{x}|}\int_s \frac{\partial\phi}{\partial n}\,dS + \frac{\mathbf{x}}{4\pi|\mathbf{x}|^3}\cdot\int_S\left(\mathbf{s}\frac{\partial\phi}{\partial n} - \mathbf{n}\phi\right)dS + O\left(\frac{1}{|\mathbf{x}|^3}\right). \tag{5.7}$$

The first quantity is the source strength

$$m(t) = -\int_s \frac{\partial\phi}{\partial n}\,dS, \tag{5.8}$$

while the second term is the far-field dipole strength $\mathbf{d}(t)$, given by

$$\mathbf{d}(t) = \int_s\left(\mathbf{n}\phi - \mathbf{s}\frac{\partial\phi}{\partial n}\right)dS. \tag{5.9}$$

Thus we may write

$$\phi \sim \frac{-m(t)}{4\pi|\mathbf{x}|} - \frac{\mathbf{d}(t)\cdot\mathbf{x}}{4\pi|\mathbf{x}|^3} + O\left(\frac{1}{|\mathbf{x}|^3}\right) \tag{5.10}$$

as a representation of the bubble in the far-field.

In addition, for an *infinite* fluid, we may also express the dipole strength in terms of the motion of the centroid and the Kelvin impulse as follows:

$$\mathbf{d}(t) = \frac{d}{dt}(V_b\mathbf{x}_c) + \frac{1}{\rho}\mathbf{I}. \tag{5.11}$$

However these relations will be modified for a *semi-infinite* fluid because of the necessary changes to the Green's function so that the boundary conditions on the half-space boundary can be satisfied. We delay further discussion of relations such as (5.11) until the next section, when the known Green's functions (or point source solutions) have been defined.

6. Point source solutions

After the derivation and physical discussion of the previous two sections, we move to exploit the option of evaluating the impulse over the half-space boundary. In a quite simple way, we may approximate the dominant motion of a cavitation bubble by a source. If we also allow the bubble to translate, we may also include a dipole. Recently Kucera and Blake [8] have developed a low-order singularity method (LOSM), consisting of a source and a dipole to model the growth and collapse of clouds of bubbles most effectively, with the theory only breaking down late in the collapse phase.

A number of point source solutions near a half-space boundary are well-known ([3]). Several of these are listed below. In all the examples, we consider a source of time-varying strength $m(t)$, a distance h from the plane boundary defined by $x = 0$.

https://doi.org/10.1017/S0334270000006111 Published online by Cambridge University Press

(i) Rigid boundary. The boundary condition for no flux through the boundary is

$$\frac{\partial \phi}{\partial x} = 0 \quad \text{on } x = 0. \tag{6.1}$$

The expression for the potential ϕ_s is

$$\phi_s = \frac{-m}{4\pi}\left[\frac{1}{((x-h)^2+r^2)^{1/2}} + \frac{1}{((x+h)^2+r^2)^{1/2}}\right]. \tag{6.2}$$

The general expression for a dipole of vector strength (d_x, d_y, d_z) is

$$\begin{aligned}\phi_d = &-\frac{d_x}{4\pi}\left[\frac{x-h}{((x-h)^2+r^2)^{3/2}} - \frac{(x+h)}{((x+h)^2+r^2)^{3/2}}\right] \\ &-\frac{d_y}{4\pi}\left[\frac{y}{((x-h)^2+r^2)^{3/2}} + \frac{y}{((x+h)^2+r^2)^{3/2}}\right] \\ &-\frac{d_z}{4\pi}\left[\frac{z}{((x-h)^2+r^2)^{3/2}} + \frac{z}{((x+h)^2+r^2)^{3/2}}\right],\end{aligned} \tag{6.3}$$

where $r = (y^2+z^2)^{1/2}$ is the radius in cylindrical polar coordinates.

It is possible to extend the ideas developed by Lighthill [10] to a semi-infinite fluid. The Green's formula for the potential near a rigid boundary is

$$\phi = \frac{1}{4\pi}\int_S \left(\frac{\partial \phi}{\partial n} G - \phi \frac{\partial G}{\partial n}\right) dS, \tag{6.4}$$

where the Green's function G in this case is defined by

$$G = 1/|\mathbf{x}-\mathbf{s}| + 1/|\mathbf{x}-\mathbf{s}'|, \tag{6.5}$$

where $\mathbf{s}$ is the position vector of a point on the bubble surface and $\mathbf{s}'$ is the position vector of the image point in the $x = 0$ plane boundary.

In an analogous way to Section 5, the far-field approximations become

$$G = \frac{2}{|\mathbf{x}|} + \frac{(\mathbf{s}+\mathbf{s}')\cdot\mathbf{x}}{|\mathbf{x}|^3} + O\left(\frac{1}{|\mathbf{x}|^3}\right), \tag{6.6}$$

and

$$\frac{\partial G}{\partial n} = \frac{2\mathbf{n}\cdot\mathbf{x}}{|\mathbf{x}|^3} + O\left(\frac{1}{|\mathbf{x}|^3}\right). \tag{6.7}$$

This leads to the following far-field expression for ϕ:

$$\phi = \frac{1}{2\pi|\mathbf{x}|}\int_s \frac{\partial \phi}{\partial n}\, dS + \frac{\mathbf{x}}{2\pi|\mathbf{x}|^3}\int_s \left\{\frac{1}{2}(\mathbf{s}+\mathbf{s}')\frac{\partial \phi}{\partial n} - \phi\mathbf{n}\right\} dS + O\left(\frac{1}{|\mathbf{x}|^3}\right). \tag{6.8}$$

In other words, the source field is twice as strong in the far-field because of the zero flux through the rigid boundary, while the dipole field is given by

$$\mathbf{d}(t) = 2\int_s \left\{\phi\mathbf{n} - \frac{1}{2}(\mathbf{s}+\mathbf{s}')\frac{\partial \phi}{\partial n}\right\} dS. \tag{6.9}$$

https://doi.org/10.1017/S0334270000006111 Published online by Cambridge University Press

If we restrict ourselves to axisymmetric motion in the x-direction (i.e. normal to the rigid boundary) we have that

$$(\mathbf{s} + \mathbf{s}') \cdot \mathbf{e}_x = 0,$$

leading to

$$d_x(t) = 2 \int_s (\phi(\mathbf{n} \cdot \mathbf{e}_x))\, dS; \tag{6.10}$$

that is,

$$d_x(t) = \frac{2}{\rho} I_x(t), \tag{6.11}$$

yielding a far-field behaviour for the potential ϕ of

$$\phi = -\frac{m(t)}{2\pi|\mathbf{x}|} - \frac{d_x(t)x}{2\pi\rho|\mathbf{x}|^3} + O\left(\frac{1}{|\mathbf{x}|^3}\right). \tag{6.12}$$

The Kelvin impulse is thus associated with the equivalent of translational motion in the far-field (i.e. a dipole).

(ii) Free surface (zero potential). The expression for a source is

$$\phi_s = \frac{-m}{4\pi}\left[\frac{1}{((x-h)^2+r^2)^{1/2}} - \frac{1}{((x+h)^2+r^2)^{1/2}}\right], \tag{6.13}$$

while for a dipole,

$$\begin{aligned}\phi_d = {} & \frac{d_x}{4\pi}\left[\frac{x-h}{((x-h)^2+r^2)^{3/2}} + \frac{x+h}{((x+h)^2+r^2)^{3/2}}\right] \\ & - \frac{d_y}{4\pi}\left[\frac{y}{((x-h)^2+r^2)^{3/2}} - \frac{y}{((x+h)^2+r^2)^{3/2}}\right] \\ & - \frac{d_z}{4\pi}\left[\frac{z}{((x-h)^2+r^2)^{3/2}} - \frac{z}{((x+h)^2+r^2)^{3/2}}\right].\end{aligned} \tag{6.14}$$

(iii) Two-fluid interface. The linearised dynamic boundary condition on the interface at $x = 0$ is

$$\rho_1\phi_1 = \rho_2\phi_2, \tag{6.15}$$

where 1 refers to the lower fluid and 2, the upper fluid. If the source is in the fluid of density ρ_1, the expressions for the potential in both fluids are as follows:

$$\phi_{1S} = \frac{-m}{4\pi}\left[\frac{1}{((x-h)^2+r^2)^{1/2}} - \frac{\rho_1-\rho_2}{\rho_1+\rho_2}\frac{1}{((x+h)^2+r^2)^{1/2}}\right] \tag{6.16}$$

$$\phi_{2S} = \frac{-m}{2\pi}\frac{\rho_1}{\rho_1+\rho_2}\frac{1}{((x-h)^2+r^2)^{1/2}}, \tag{6.17}$$

https://doi.org/10.1017/S0334270000006111 Published online by Cambridge University Press

and for a dipole

$$\begin{aligned}\phi_{1d} = &-\frac{d_x}{4\pi}\left[\frac{x-h}{((x-h)^2+r^2)^{3/2}}+\frac{\rho_1-\rho_2}{\rho_1+\rho_2}\frac{x+h}{((x+h)^2+r^2)^{3/2}}\right]\\ &-\frac{d_y}{4\pi}\left[\frac{y}{((x-h)^2+r^2)^{3/2}}-\frac{\rho_1-\rho_2}{\rho_2+\rho_2}\frac{y}{((x+h)^2+r^2)^{3/2}}\right]\\ &-\frac{d_z}{4\pi}\left[\frac{z}{((x-h)^2+r^2)^{3/2}}-\frac{\rho_1-\rho_2}{\rho_1+\rho_2}\frac{z}{((x+h)^2+r^2)^{3/2}}\right]\end{aligned} \tag{6.18}$$

$$\begin{aligned}\phi_{1S} = &\frac{d_x}{4\pi}\frac{\rho_1}{\rho_1+\rho_2}\frac{x-h}{((x-h)^2+r^2)^{3/2}}-\frac{d_y}{4\pi}\frac{\rho_1}{\rho_1+\rho_2}\frac{y}{((x-h)^2+r^2)^{3/2}}\\ &-\frac{d_z}{4\pi}\frac{\rho_1}{\rho_1+\rho_2}\frac{z}{((x-h)^2+r^2)^{3/2}}.\end{aligned} \tag{6.19}$$

(iv) Inertial boundary. As a model for an inertial boundary we suppose a material of mass per unit area σ forms the boundary, but with no rigidity. The kinematic condition for $\zeta(r,t)$, the displacement of the boundary, is

$$\frac{\partial\zeta}{\partial t}=\frac{\partial\phi}{\partial x} \quad \text{on } x=0. \tag{6.20}$$

The linearised dynamic boundary condition for an inertial boundary is

$$\sigma\frac{\partial^2\zeta}{\partial t^2}=p_\infty-p. \tag{6.21}$$

When the linearised Bernoulli pressure condition of

$$p=p_\infty-\rho\frac{\partial\phi}{\partial t} \tag{6.22}$$

is substituted into (6.21) and integrated, the following mixed boundary condition is obtained:

$$\sigma\frac{\partial\phi}{\partial x}-\rho\phi=0 \quad \text{on } x=0. \tag{6.23}$$

The point source solution for this boundary condition is

$$\begin{aligned}\phi_S = -\frac{m}{4\pi}\Bigg[&\frac{1}{[(x-h)^2+r^2]^{1/2}}+\frac{1}{[(x+h)^2+r^2]^{1/2}}\\ &-2\rho/\sigma\int_0^\infty\frac{e^{-\xi(x+h)}}{\xi+\rho/\sigma}J_0(\xi r)\,d\xi\Bigg],\end{aligned} \tag{6.24}$$

https://doi.org/10.1017/S0334270000006111 Published online by Cambridge University Press

and the dipole is,

$$\begin{aligned}\phi_d = -\frac{d_x}{4\pi}\Bigg[&\frac{x-h}{((x-h)^2+r^2)^{3/2}} - \frac{(x+h)}{((x+h)^2+r^2)^{3/2}} \\ &-2\rho/\sigma\int_0^\infty \frac{\xi e^{-\xi(x+h)}}{\xi+\rho/\sigma}J_0(\xi r)\,d\xi\Bigg] \\ -\frac{d_y}{4\pi}\Bigg[&\frac{y}{[(x-h)^2+r^2]^{3/2}} + \frac{y}{[(x+h)^2+r^2]^{3/2}} \\ &-2\rho/\sigma\frac{y}{r}\int_0^\infty \frac{\xi e^{-\xi(x+h)}}{\xi+\rho/\sigma}J_1(\xi r)\,d\xi\Bigg] \\ -\frac{d_z}{4\pi}\Bigg[&\frac{z}{((x-h)^2+r^2)^{3/2}} + \frac{z}{((x+h)^2+r^2)^{1/2}} \\ &-2\rho/\sigma\frac{z}{r}\int_0^\infty \frac{\xi e^{-\xi(x+h)}}{\xi+\rho/\sigma}J_1(\xi r)\,d\xi\Bigg],\end{aligned} \tag{6.25}$$

where J_0 is a Bessel function of first kind and zeroth order.

(v) Membrane boundary. As a model for a boundary with both inertia and a restoring force we consider a membrane boundary which satisfies the kinematic relation (6.20) and dynamic relation for the displacement $\varsigma(r,t)$ as follows:

$$\sigma\frac{\partial^2\varsigma}{\partial t^2} - T\nabla_r^2\varsigma = p_\infty - p, \tag{6.26}$$

where σ is the mass per unit area and T the tension in the membrane. Using the linearised Bernoulli pressure condition of (6.22) leads to the following boundary condition for ϕ on the membrane:

$$\frac{\partial^2}{\partial t^2}\left(\sigma\frac{\partial\phi}{\partial x} - \rho\phi\right) - T\nabla_r^2\left(\frac{\partial\phi}{\partial x}\right) = 0. \tag{6.27}$$

The point source solution for the membrane boundary is

$$\begin{aligned}\phi_s = -\frac{m}{4\pi}\Bigg[&\frac{1}{((x-h)^2+r^2)^{1/2}} - \frac{1}{((x-h)^2+r^2)^{1/2}} \\ &-\frac{1}{2\pi}\int_0^\infty \left(\frac{T\xi^3}{\rho}\right)^{1/2}(e^{-\xi(x+h)})J_0(\xi r) \\ &\times\left\{\int_0^t m(t-\tau)\sin\left(\frac{T\xi^3}{\rho}\right)^{1/2}\tau\,d\tau\right\}d\xi\Bigg].\end{aligned} \tag{6.28}$$

7. Estimates of the Kelvin impulse for a point source

The sign of the x-component of the Kelvin impulse determines whether the bubble either migrates towards or away from the boundary in much the same way

https://doi.org/10.1017/S0334270000006111 Published online by Cambridge University Press

as the impulse of a particle in (2.3). To obtain the point source representations of the previous section, we have specified the boundary conditions on the plane $x = 0$. We may also evaluate the x-component of the Kelvin impulse on this boundary, which reduces to the simple form

$$I_x(t) = I_{0x} + \int_0^t F_x(t)\,dt, \tag{7.1}$$

where I_{0x} is the initial Kelvin impulse in the x-direction and

$$F_x(t) = \rho\pi \int_0^\infty r(u^2 - v^2)\,dr \tag{7.2}$$

with u and v being the velocities on $x = 0$ in the x and r directions respectively. Calculating the initial Kelvin impulse for singularities poses some difficulties, because we have not specified the surface S. However if we choose S to be a sphere of very small radius R and take the limit as R tends to zero in the integral definition (3.1) for the Kelvin impulse, we find that

$$I_{0x} = \begin{cases} 0 & \text{source} \\ \frac{1}{3}d_x(0) & \text{dipole,} \end{cases} \tag{7.3}$$

where $d_x(0)$ is the initial dipole strength and where higher order singularities are undefined because they are too singular (i.e. $dS = O(R^2), \phi_n = O(1/R^n), n = 1$ for a source, $n = 2$ for a dipole, $n > 2$ undefined). From (5.11) it may be deduced that the remaining 2/3 of the dipole strength comes from the time rate of change of $V_b\mathbf{x}_c$. Of course, in practice, the initial condition for the bubble may be one of finite size in which case the above statement would not be applicable, although (7.3) would remain correct to first order for a bubble near a boundary. Indeed if we considered a finite spherical bubble of initial radius R_0 and velocity $\mathbf{U}_0$, in an infinite fluid the well-known potential is given by

$$\phi = -R_0^3\mathbf{U}_0 \cdot \mathbf{x}/(2|\mathbf{x}|^3), \tag{7.4}$$

a potential produced by a dipole of strength $\mathbf{d} = 2\pi R_0^3\mathbf{U}_0$. Thus the initial Kelvin impulse [10] in this case is

$$\mathbf{I}_0 = (2\pi/3)\rho R_0^3\mathbf{U}_0 = (1/2)\rho V_b\mathbf{U}_0. \tag{7.5}$$

The quantity $\frac{1}{2}\rho V_b$ is often referred to as the added mass of a bubble in an infinite fluid. For a bubble in an effectively infinite medium, the Kelvin impulse will remain constant, equal to $\mathbf{I}_0$ in (7.5).

Upon substitution of the respective gradients of the potential ϕ into (7.2), we obtain the following values for $F_x(t)$ corresponding to the listed boundaries.

(i) Rigid boundary.

$$F_x(t) = -\rho m^2/(16\pi h^2). \tag{7.6}$$

https://doi.org/10.1017/S0334270000006111 Published online by Cambridge University Press

(ii) Free surface (zero potential).

$$F_x(t) = \rho m^2/(16\pi h^2). \tag{7.7}$$

(iii) Two-fluid interface.

$$F_x(t) = \rho_1 m^2(\rho_1 - \rho_2)/(16\pi h^2(\rho_1 + \rho_2)). \tag{7.8}$$

(iv) Inertial boundary.

$$F_x(t) = (\rho m^2)/(4\pi h^2)H(\alpha), \tag{7.9}$$

where

$$H(\alpha) = \alpha - 1/4 - 2\alpha^2 e^{2\alpha} E_1(2\alpha), \tag{7.10}$$

with the non-dimensional parameter α defined as $\alpha = \rho h/\sigma$ and E_1 an exponential integral, as in [1]. The limit as α tends to zero corresponds to the rigid boundary limit (i.e. infinite mass for the boundary), while α tending to infinity yields the free surface (zero potential) result.

For the case of the inertial boundary it is also possible to include a dipole $d(t)$ for the axisymmetric case. This yields the following expression for $F_x(t)$:

$$F_x(t) = \frac{\rho}{4\pi h^2}\left[m^2 H(\alpha) - \frac{md}{h}G(\alpha) + \frac{d^2}{h^2}F(\alpha)\right], \tag{7.11}$$

where the additional expressions $G(\alpha)$ and $F(\alpha)$ are defined as follows:

$$G(\alpha) = -1/2 + \alpha - 2\alpha^2 + 4\alpha^3 e^{2\alpha} E_1(2\alpha) \tag{7.12}$$

$$F(\alpha) = -3/8 + 1/2\alpha - 1/2\alpha^2 + \alpha^3 - 2\alpha^4 e^{2\alpha} E_1(2\alpha). \tag{7.13}$$

Graphical representations of $H(\alpha)$, $G(\alpha)$ and $F(\alpha)$ are illustrated in Figure 2. It is of interest to note that the contributions to the Kelvin impulse from the source term do not depend on whether it is acting as a source or a sink (i.e. $F_x \propto m^2$). In addition it depends on the inverse square of the distance from the boundary. Thus the closer the bubble is to the boundary, the greater the impulse. Clearly it would be desirable, in terms of increasing the impulse, if the bubbles were attracted towards the boundary, corresponding to $F_x < 0$. On the other hand one of our prime objectives would be to reduce the Kelvin impulse and the potential for causing physical damage to the boundary. This would result if $F_x > 0$, leading to the bubbles migrating away from the boundary.

(v) Membrane boundary.

$$F_x(t) = \frac{\rho}{4\pi h^2}\left[m^2 H(\alpha) - 2\sum_{n=0}^{\infty} \frac{\alpha^{2n+4} c^{2n+2} e^{2\alpha}}{(2n+1)! h^{2n+2}} B_n(2\alpha) \int_0^t (t-\tau)^{2n+1} m(\tau) m(t)\, d\tau\right], \tag{7.14}$$

https://doi.org/10.1017/S0334270000006111 Published online by Cambridge University Press

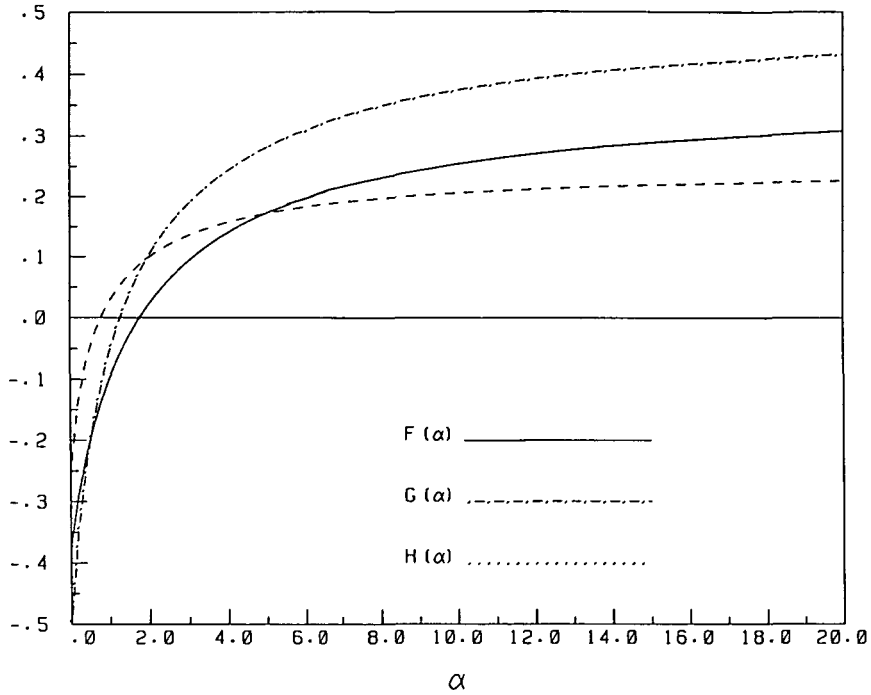

FIGURE 2. Graphs of the functions $H(\alpha)$, $G(\alpha)$ and $F(\alpha)$ where $\alpha = \rho h/\sigma$.

where $c = (T/\sigma)^{1/2}$ is the wave speed of the membrane and $B_n(2\alpha)$ consists of a finite sum of exponential integrals. It is of interest to note that this boundary has "memory" effects in that it can extract or inject energy back into the fluid. This is realised in moment-like terms on the RHS of (7.14). In all of these expressions for $F_x(t)$, a term equal to $\rho g V(t) \cos\theta$ representing buoyancy forces may be added. Later we shall use this extra term when trying to assess the relative importance of buoyancy forces when comparing this theory against both experimental results and numerical simulations.

8. Estimates of the final Kelvin impulse for a bubble

To develop the theory further, it is convenient to scale all length dimensions with respect to R_m, the maximum bubble radius, and time with respect to $R_m/(\Delta p)^{1/2}$ where Δp is the pressure difference between the initial pressure p_0 in the fluid at the location of the bubble prior to it being generated and the vapour pressure p_c inside the bubble (i.e. $\Delta p = p_0 - p_c$). This leads to the

https://doi.org/10.1017/S0334270000006111 Published online by Cambridge University Press

definition of the dimensionless parameter,

$$\gamma = h/R_m,$$

which is the specification of the initial location of the bubble centroid.

In the previous section, values of $F_x(t)$ were obtained for point source solutions near different boundaries. To obtain the final Kelvin impulse (i.e. the Kelvin impulse at completion) we need an expression $m(t)$. If the bubble centroid is located at a sufficient distance from the boundary (i.e. $\gamma \gg 1$), the bubble will remain almost spherical allowing us to use the expression for $m(t)$ from the Rayleigh bubble solution for a cavitation bubble in an infinite fluid. Thus the source strength $m(t)$ becomes

$$m(t) = \frac{dV}{dt} = 4\pi R^2 \dot{R}, \tag{8.1}$$

where

$$\dot{R}^2 = \frac{2}{3}\left(\frac{1}{R^3} - 1\right) \tag{8.2}$$

may be obtained by integration of the dynamic boundary condition on the surface of the bubble. This may be substituted into the relevant equations in Section 7 to yield the final Kelvin impulse as follows:

$$I_x(T_c) = \int_0^{T_c} F_x(t)\, dt, \tag{8.3}$$

where T_c is equal to the lifetime of the Rayleigh bubble ($T_c = 1.83\ldots$). We postulate that when $I_x(T_c)$ is less than zero, the bubble migrates towards the boundary. Conversely if $I_x(T_c)$ is greater than zero the bubble will migrate away from the boundary. On the other hand a near zero value of $I_x(T_c)$ would indicate the case of a "neutral" bubble when virtually no translation occurs.

If we include buoyancy forces we need to define an additional dimensionless parameter δ given by

$$\delta = (\rho g R_m/\Delta p)^{1/2}, \tag{8.4}$$

where g is the gravitational acceleration.

The general dimensional expression for (8.3) is

$$I_x(T_c) = 2\pi\sqrt{6}R_m^5(\Delta p\rho)^{1/2}/(9h^2)[2\gamma^2\delta^2 B(11/6, 1/2)\cos\theta + \chi B(7/6, 3/2)], \tag{8.5}$$

where

$$\chi = \begin{cases} -1 & : \text{ Rigid boundary} \\ +1 & : \text{ Free surface} \\ H(\alpha) & : \text{ Inertial boundary} \\ (\rho_1 - \rho_2)/(\rho_1 + \rho_2) & : \text{ Two-fluid interface,} \end{cases} \tag{8.6}$$

and θ may be either 0 or π (i.e. the boundary is below the bubble (0), or above the bubble (π)). $B(x, y)$ is a beta function (see e.g. [1]). Clearly $I_x(T_c)$ may

https://doi.org/10.1017/S0334270000006111 Published online by Cambridge University Press

be either positive or negative depending on the direction of the buoyancy force and the type of boundary. We now consider four cases where competing effects prevail and where some comparison with experiment or numerical simulation is available.

(i) Buoyant bubble near a rigid boundary. Omitting the dimensional terms in (8.5), the expression for the Kelvin impulse [5] at completion for a cavitation bubble near a rigid boundary for $\theta = 0$ is

$$I_x(T_c) \propto [2\gamma^2\delta^2 B(11/6, 1/2) - B(7/6, 3/2)]. \tag{8.7}$$

Following the arguments presented earlier, if $I_x(T_c) > 0$ the bubble will migrate away from the rigid boundary; for $I_x(T_c) < 0$, the bubble will migrate towards the rigid boundary. The null impulse line corresponds to $I_x(T_c) = 0$ yielding the following relation between the parameters:

$$\gamma\delta = [B(7/6, 3/2)/2B(11/6, 1/2)]^{1/2} = 0.442. \tag{8.8}$$

In Figure 3, this prediction for determining the migration characteristics of a cavitation bubble near a rigid boundary [5] is tested out against a number of numerical simulations for different values of (γ, δ). Although only a limited set of simulations have been conducted it does appear to be a reliable estimator of the migratory behaviour of bubbles.

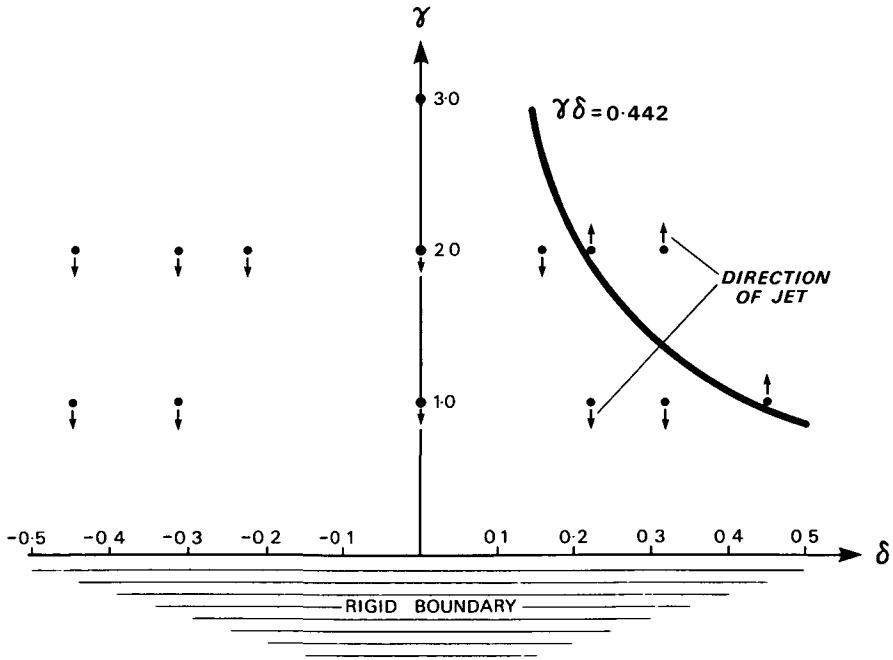

FIGURE 3. The $\gamma - \delta$ parameter space for buoyant vapour bubbles near a rigid boundary [5]. Numerical predictions are included for specific (γ, δ) examples.

https://doi.org/10.1017/S0334270000006111 Published online by Cambridge University Press

(ii) Buoyant bubble near a free surface. In a strict sense we should also include a gravity term in the free surface boundary condition as was done in Blake, Taib and Doherty [6]. However the lowest order approximation can be obtained from the zero potential boundary condition because the dominant term is the buoyancy of the bubble, not the gravitational restoring force on the free surface, especially when $\gamma \gg 1$. Thus the expression for $I_x(T_c)$ near a free surface with $\theta = \pi$ becomes

$$I_x(T_c) \propto [-2\gamma^2\delta^2 B(11/6, 1/2) + B(7/6, 3/2)], \tag{8.9}$$

leading to exactly the same relation between the γ and δ parameters as for a rigid boundary, albeit in this case the bubble is repelled by the free surface and the boundary is on the uppermost side of the bubble (the coordinate system of Figure 1 has been rotated through π).

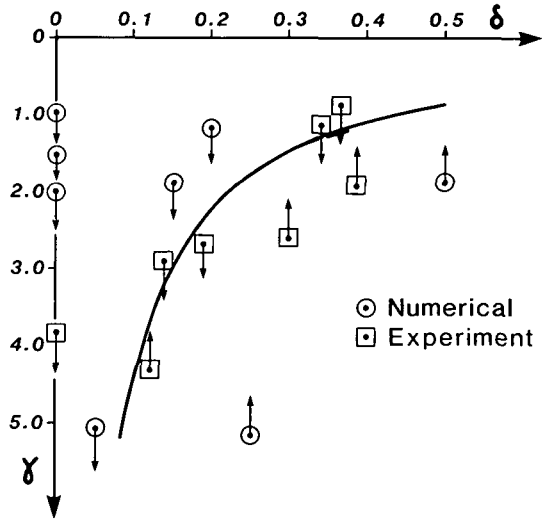

FIGURE 4. The (γ, δ) parameter space for buoyant bubbles near a free surface [6]. Both numerical predictions and experimental observations are included on the graph.

In Figure 4, comparisons are made between both the experimental observations of Dr. D. C. Gibson and the numerical simulations of Blake, Taib and Doherty [6]. Again the Kelvin impulse appears to be a remarkable predictor of the likely migratory response of a cavitation bubble near a free surface.

(iii) Two-fluid interface. This is similar to the free surface example in that

$$I_x(T_c) \propto \left[-2\gamma^2\delta^2 B\left(\frac{11}{6}, \frac{1}{2}\right) + \frac{\rho_1 - \rho_2}{\rho_1 + \rho_2} B\left(\frac{7}{6}, \frac{3}{2}\right)\right], \tag{8.10}$$

where δ needs to slightly modified to $\delta = (\rho_1 g R_m/\Delta p)^{1/2}$. Equating (8.10) to zero yields the following relationship between γ and δ for the null impulse line:

$$\gamma\delta = 0.442[\rho_1 - \rho_2)/(\rho_1 + \rho_2)]^{1/2}. \tag{8.11}$$

https://doi.org/10.1017/S0334270000006111 Published online by Cambridge University Press

Chahine and Bovis [7] show several results for bubbles near a water-white spirit interface. For $\gamma = 2.2$ the bubble moves towards the interface, suggesting buoyancy forces dominate, while for $\gamma = 0.87$ the bubble is repelled by the interface, suggesting the interface interaction dominates. It is not possible to make a more accurate comparison because of a lack of further details on the experimental arrangements.

(iv) Inertial boundary, no translation or buoyancy. In the case of no translation and negligible buoyancy forces, we set $\delta = 0$. The expression for the Kelvin impulse now becomes

$$I_x(T_c) \propto H(\alpha) \tag{8.12}$$

where $\alpha = \rho h/\sigma$. $H(\alpha)$ is equal to zero when

$$\alpha = \alpha_0 = 0.7798\ldots \tag{8.13}$$

Recently Shima and Tomita [12] have conducted experiments on the growth and collapse of a cavitation bubble near a composite surface consisting of a thin sheet of rubber covering a layer of foam (see Figure 1). They concluded that the "bubble migration depends not only on the characteristics of the boundary surfaces but also on the position of the bubble from the surface". Comparisons can be made with the Shima and Tomita results, although our comparisons are restricted to their "neutral collapse" cases when there is no translation of the bubble. This would correspond to a null Kelvin impulse in our theory. After rearranging, it is possible to show that the ratio of two quantities (h/R_m and t_R) measured by Shima and Tomita should be constant, i.e.

$$(h/R_m)/t_R = \alpha_0 \rho_R/(\rho R_m), \tag{8.14}$$

where t_R is the thickness and ρ_R the density of the rubber sheet respectively. In theory the RHS of (8.14) should be constant (and hence also the LHS) because both the density of the liquid and the rubber are constant (the compressibility would occur in the light weight foam) together with R_m being constant. The results for the three cases obtained by Shima and Tomita [12] are tabulated below:

$t_R(mm)$	(h/R_m)	$(h/R_m)/t_R$
3.0	1.31	0.44
4.0	1.66	0.42
5.0	2.11	0.42

Even though this theory is restrictive in that it is linear theory, there does appear to be a relatively close comparison with experiment for these few cases.

https://doi.org/10.1017/S0334270000006111 Published online by Cambridge University Press

9. Conclusions

It is clear that the Kelvin impulse can provide us with extensive "physical insight" into the anticipated behaviour of cavitation bubbles near different boundaries. Furthermore, it also appears to provide us with remarkably accurate prediction of the gross response characteristics of a bubble near a boundary without the need to develop sophisticated numerical simulation schemes [5, 6]. It is likely that these ideas can be extended to multi-bubble and bubble-cloud simulations.

Acknowledgements

The author acknowledges the contributions and encouragement that Dr. D. C. Gibson of the CSIRO Division of Energy Technology has given continuously to this research. This paper is based on a lecture presented to the Institute of High Speed Mechanics, Tohoku University, Japan in July 1987. The author also wishes to express his grateful thanks to Professor A. Shima and Dr. Y. Tomita for providing details of their most recent experiments on cavitation bubbles near composite surfaces. Acknowledgement is also made to the Australian Research Grants Scheme for supporting the research programme on cavitation bubble dynamics near boundaries.

References

[1] M. Abramowitz and I. A. Stegun, *Handbook of Mathematical Functions* (Dover, N. Y. 1965).

[2] T. B. Benjamin and A. T. Ellis, "The collapse of cavitation bubbles and the pressures thereby produced against solid boundaries", *Phil. Trans. R. Soc. London. Ser. A* **260** (1966) 221–40.

[3] J. R. Blake and P. Cerone, "A note on the impulse due to a vapour bubble near a boundary", *J. Aust. Math. Soc.* **23** (1982) 383–393.

[4] J. R. Blake and D. C. Gibson, "Cavitation bubbles near boundaries", *Ann. Rev. Fluid Mech.* **19** (1987) 99–123.

[5] J. R. Blake, B. B. Taib and G. Doherty, "Transient cavities near boundaries. Part 1. Rigid Boundary", *J. Fluid Mech.* **170** (1986) 479–497.

[6] J. R. Blake, B. B. Taib and G. Doherty, "Transient cavities near boundaries Part 2. Free Surface", *J. Fluid Mech.* **181** (1987) 197–212.

[7] G. L. Chahine and A. Bovis, "Oscillations and collapse of a cavitation bubble in the vicinity of a two-liquid interface." in *Cavitation and inhomogeneities in underwater acoustics* (ed. W. Lauterborn) (Springer, Berlin, 1980).

[8] A. Kucera and J. R. Blake, "Computational modelling of cavitation bubbles near boundaries." in *Commutational Techniques and Applications CTAC-87* (eds. J. Noye and C. Fletcher) (North Holland, Amsterdam, 1988) 391–400.
[9] H. Lamb, *Hydrodynamics* (CUP, Cambridge, 1930).
[10] J. Lighthill, *An Informal Introduction to Theoretical Fluid Mechanics* (O.U.P. Oxford, 1986).
[11] A. Prosperetti and D. Manzi, "Mechanism of jet formation for a translating and collapsing bubble", (submitted 1987).
[12] A. Shima and Y. Tomita, Private communication (1987).